Current Titles

National Center for Electron Microscopy

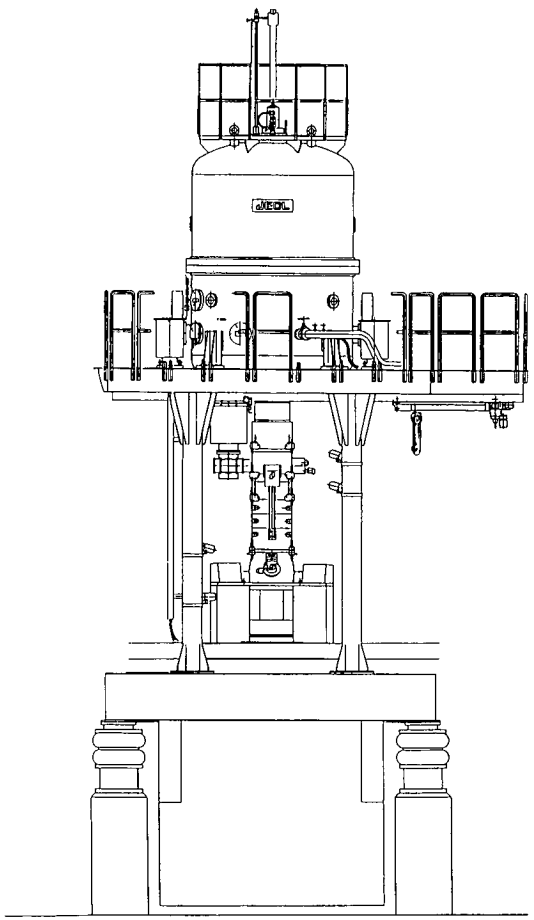

April 1997

National Center for Electron Microscopy
Berkeley Laboratory
1 Cyclotron Rd., Building 72
Berkeley CA 94720

National Center for Electron Microscopy
Berkeley Laboratory
1 Cyclotron Rd., Building 72
Berkeley CA 94720

Please send a reprint of the paper(s):

Number	First Author	Title (first two words)

Name_____ Date_____

Affiliation _____

Address _____

_____

Please send a reprint of the paper(s):

Number	First Author	Title (first two words)

Name_____ Date_____

Affiliation _____

Address _____

_____

Current Titles

National Center for Electron Microscopy
Ernest Orlando Lawrence
Berkeley National Laboratory
University of California
Berkeley, California 94720

April 1997

PUB-719

For current information about the NCEM
see our www page at
http://ncem.lbl.gov/ncem.html

The NCEM is supported by the Director, Office of Energy Research, Office of Basic Energy Sciences, Materials Sciences Division of the U.S. Department of Energy under Contract No. DE-AC03-76SF00098.

This booklet is published for those interested in current research being conducted at the National Center for Electron Microscopy. The NCEM is a DOE-designated national user facility and is available at no charge to qualified researchers. Access is controlled by an external steering committee. Interested researchers may contact Gretchen Hermes at (510) 486-5006 or address below for a User's Guide.

Copies of available papers in print may be ordered by their publication number using the enclosed order cards.

Articles are listed alphabetically by journal

Pub 475 ■ **NCEM User's Guide**

NCEM User's Guide *1993*

User's guide to the National Center for Electron Microscopy, Lawrence Berkeley Laboratory, University of California, Berkeley.

Pub 658 ■ **NCEMSS Manual**

M.A. O'Keefe and R. Kilaas

NCEMSS Software Manual *1994*

Manual for the National Center for Electron Microscopy Simulation System for the simulation of HRTEM images.

---

no # ■ **Role of Arsenic Antisite Defect in Nonstoichiometric Gallium Arsenide**

J. Jasinski, A. Kurpiewski, K. Korona, M. Kaminska, Z. Liliental-Weber

Acta Physica Polonica A 88 747-50

Over the last few years there have been many studies of GaAs layers grown at low temperatures (180-300°C), so called LTGaAs. The interest in LT GaAs was motivated by the potential application of 600°C annealed LT GaAs in microwave and fast optoelectronic devices because of its short photocarrier lifetime, reasonable mobility and high resistivity. These properties are associated with the nonstoichiometry of LT GaAs. Recently, studies of comparable material, nonstoichiometric GaAs produced by arsenic ion implantation have been initiated. There is still a strong controversy as to whether the arsenic antisite (As_{Ga}) or arsenic precipitates are responsible for unique electrical properties of both materials. This paper presents the results of structural and electrical studies of high energy As implanted GaAs and comments on relationships between the structure and the resulting electrical properties.

---

no # ■ **HRTEM of Microcrystalline Opal in Chert and Porcelanite from the Monterey Formation, California**

S.L. Cady, H.R. Wenk, and K.H. Downing

American Mineralogist 81 1380-13 *1996*

Microcrystalline opal was investigated using low-dose transmission electron microscopy (TEM) methods to identify microstructural characteristics and possible phase transformation mechanisms that accommodate silica diagenesis. High-resolution TEM (HTREM) revealed that microcrystalline opal in opal-CT chert (>90 wt% silica) and opal-CT porcelanite (50-90 wt% silica) from the Miocene Monterey Formation of California displays various amounts of structural disorder and coherent and incoherent lamellar intergrowths. Species of microfibrous opal identified by HRTEM in early formed opal-CT chert include length-slow opal-C and unidimensionally disordered length-slow opal-CT ("lussatite"). These fibers often display a microstructure characterized by an aperiodic distribution of highly strained domains that separate ordered domains located at discrete positions along the direction of the fiber axes, TEM revealed that the siliceous matrix in later-formed opal-CT porcelanite consists of equidimensional, nanometer-size opal-CT crystallites and lussatite fibers. Pseudo-orthorhombic tridymite (PO-2) was identified by HRTEM in one sample of opal-CT porcelanite.

37885 ■ **Quasi-one-dimensional CaF_2 Islands Formed on Si(001) by Molecular Beam Epitaxy**

D. Loretto, F.M. Ross and C.A. Lucas

Appl. Phys. Lett. 68 2363 *1996*

Quasi-one-dimensional CaF_2 islands, 5-10 nm in both width and height and several μm in length, have been grown on Si(001) by molecular beam epitaxy. Using conventional and high resolution transmission electron microscopy, we show that the islands grow in two symmetry-equivalent orientations and are bounded by {111} facets. The unusual island morphology is attributed to a low density of nucleation sites, the small lattice mismatch and the anisotropic CaF_2 surface energy.

38375 ■ **Recrystallization of High Energy As-implanted GaAs Studied by Transmission Electron Microscopy**

J. Jasinski, Y. Chen, J. Washburn, Z. Liliental-Weber, H.H. Tan, C. Jagadish and M. Kaminska

Appl. Phys. Lett. 68 1501-15 *1996*

Ion implantation damage and the regrowth process during thermal annealing of 2 MeV As-ion-implanted GaAs were studied by transmission electron microscopy. With low-temperature annealing, a high density of stacking faults was formed during the recrystallization process, but they were rarely observed with high-temperature annealing. At intermediate temperatures, a much lower density of stacking faults was generated at the upper interface between the buried amorphous layer and the crystal than that at the lower interface, where a higher concentration of As-implanted arsenic exists. Based on the observed experimental results, an atomic model is proposed to explain the formation of stacking faults induced by As clusters.

38101 □ **Nucleation and Evolution of Misfit Dislocations in ZnSe/GaAs(001) Heterostructures Grown by Low-Pressure Organometallic Vapor Phase Epitaxy**

S. Ruvimov, E. Bourret, J. Washburn and Z. Liliental-Weber

Appl. Phys. Lett. 68 3346-34 *1996*

Transmission electron microscopy and x-ray diffraction were used to study strain relaxation and the evolution of the dislocation structure in ZnSe epilayers grown by low-pressure organometallic vapor phase epitaxy on a (001) surface of semi-insulating GaAs. Before the ZnSe growth, the substrate surface was exposed to a flow of tertiarybutylarsine to promote an As-terminated surface. This surface treatment results in a low density of stacking faults; 60° misfit dislocations were observed at a layer thickness as low as 0.05 μm. This agrees well with the theoretical critical value for misfit dislocation formation in the ZnSe/GaAs system, but is much lower than experimental critical thicknesses reported earlier. Various mechanisms of misfit dislocation generation were observed at different growth stages. The evolution of the dislocation structure is discussed in relation with the morphology of the ZnSe layers.

39027 □ **Quenching of Giant Magnetoresistance by Interface Roughening and Alloying in Annealed $[(Ni_xFe_{1-x})_yAu_{1-y}]$/Au Multilayers**

R.F.C. Farrow, S.S.P. Parkin, R.F. Marks, K.M. Krishnan, K.M. and N. Thangaraj

Appl. Phys. Lett. 69 1963 *1996*

Antiferromagnetically coupled permalloy/Au multilayers display giant magnetoresistance (GMR) with large changes of resistance in very low fields. We show that thermal annealing of such structures, exhibiting GMR, leads to a quenching of the magnetoresistance. The detailed structure of the permalloy/Au interfaces has been probed using high resolution corss-section transmission electron microscopy. On annealing, the Au layers interdiffuse into the permalloy layers which leads both to rougher permalloy/Au interfaces and to "thinner" Au spacer layers. We infer that the latter results in ferromagnetic coupling of the permalloy layers which accounts for the reduced GMR.

39666 ■ Inversion Domains in GaN Grown on Sapphire

L.T. Romano, J.E. Northrup, and M.A. O'Keefe

Appl. Phys. Lett. 69 2394-23 *1996*

Planar defects observed in GaN films grown on (0001) sapphire have been identified as inversion domain boundaries (IDBs) by a combination of high resolution transmission electron microscopy, multiple dark field imagining, and convergent beam electron diffraction techniques. Films grown by molecular beam epitaxy (MBE), metalorganic vapor deposition (MOCVD), and hyride vapor phase epitaxy (HVPE) were investigated and all were found to contain IDBs. The IDBs in the MBE and HVPE films extended from the interface to the film surface and formed columnar domains that ranged in width from 3 to 20 nm in the MBE films and up to 100 nm in the HVPE films. For the films investigated, the MBE films had the highest density, and the MOCVD films had the lowest density of IDBs. The nucleation of the inversion domains (IDs) may result from step-related inhomogeneities of the GaN/sapphire interface.

38659 ■ Microstructure of Ti/Al and Ti/Al/Ni/Au Ohmic contacts for n-GaN

S. Ruvimov, Z. Liliental-Weber , J. Washburn, K.J. Duxstad, E.E. Haller

Appl. Phys. Lett. 69 1556-15 *1996*

Transmission electron microscopy has been applied to characterize the structure of Ti/Al and Ti/Al/Ni/Au Ohmic contacts on *n*-type GaN (~10^{17} cm^{-3} epitaxial layers. The metals were deposited either by conventional electron-beam or thermal evaporation techniques, and then thermally annealed at 900° C for 30 s in a N_2 atmosphere. Before metal deposition, the GaN surface was treated by reactive ion etching. A thin polycrystalline cubic TiN layer epitaxially matched to the (0001) GaN surface was detected at the interface with the GaN substrate. This layer was studied in detail by electron diffraction and high resolution elctron microscopy. The orientation relationship between the cubic TiN and the GaN was found to be: $\{111\}_{TiN}//\{00.1\}_{GaN}$, $[110]_{TiN}//[11.0]_{GaN}$, $[112]_{TiN}//[10.0]_{GaN}$. The formation of this cubic TiN layer results in an excess of N vacancies in the GaN close to the interface which is considered to be the reason for the low resistance of the contact.

38659 □ Effect of Si Doping on the Dislocation Structure of GaN Grown on the A-face of Sapphire

S. Ruvimov, Z. Liliental-Weber, T. Suski, J. Ager III, J. Washburn, et. al

Appl. Phys. Lett. 69 990-992 *1996*

Transmission electron microscopy, x-ray diffraction, low-temperature photo luminescence, and Raman spectroscopy were applied to study stress relaxation and the dislocation structure in a Si-doped GaN layer in comparison with an undoped layer grown under the same conditions by metal organic vapor phase epitaxy on (11.0) Al_2O_3. Doping of the GaN by Si to a concentration of 3 X 10^{18} cm^{-3} was found to improve the layer quality. It decreases dislocation density from 5 X 10^9 (undoped layer) to 7 X10^8 cm^{-2} and changes the dislocation arrangement toward a more random distribution. Both samples were shown to be under biaxial compressive stress which was slightly higher in the undoped layer. The stress results in a blue shift of the emission energy and E_2 phonon peaks in the photo luminescence and Raman spectra. Thermal stress was partly relaxed by bending of threading dislocations into the basal plane. This leads to the formation of a three-dimensional dislocation network and a strain gradient along the *c* axis of the layer.

39014 □ High-Resistivity and Ultrafast Carrier Lifetime in Argon Implanted GaAs

W. Walukiewicz, Z. Liliental-Weber, J. Jasinski, et. al.

Appl. Phys. Lett. 69 2569 *1996*

We have investigated the optoelectronic and structural properties of GaAs that has been implanted with Ar ions and subsequently annealed. The material exhibits all the basic optical and electronic characteristics typically observed in non-stoichiometric, As-implanted or low-temperature-grown GaAs. Annealing of Ar implanted GaAs at 600°C produces a highly resistive material with a sub-picosecond trapping lifetime for photoexcited carriers. Transmission electron microscopy shows that instead of As precipitates, characteristic for the nonstoichiometric GaAs, voids ranging in size from 3 to 5 nm are observed in Ar implanted and annealed GaAs.

no # ■ **Quantitative HRTEM: A Novel Approach Toward Application Oriented Basic Research**

C. Kisielowshi, Z. Liliental-Weber, and E. Weber

Brazilian Journal of Physics 26 83-94 *1996*

This paper reviews recent developments of microscopic methods that base on a quantitative analysis of electron micrographs to access subsurface systems at the atomic scale. It focuses on non-equilibrium diffusion processes that are observed in nanostructured MBE grown materials if a low growth temperature was used and on local deviations from a stoichiometric composition of materials. As examples we investigate GaAs/AlAs and Si/GeSi heterostructures and GaN single crystals. The purpose of the research is twofold. On the one hand it helps understanding physical processes at the atomic scale. On the other hand we can use the results to link basic physical knowledge with the performance of semiconductor devices made from nanostructured materials.

39494 ■ **Collapsing Carbon Nanotubes with an Electron Beam**

N.G. Chopra, F.M. Ross and A. Zettl

Chem. Phys. Lett. 256 241-245 *1996*

We report the first in situ study of the dynamical behavior of carbon nanotubes. We have used high energy electrons to collapse multi-walled tubes in an atomic resolution transmission electron microscope. Our video recorded observations show the real time dynamics of collapse of the tubular structure. We propose that the orientation dependent damage and channeling effects of the incident 800 keV electrons enable the multi-walled tube to flatten parallel to the flow of electrons. Evidence is seen for a zipper-like closure effect initiated by van der Waals interactions between the inner tube walls.

37581 □ **Sorption Mechanisms of Lanthanum on Oxide Minerals**

S. Fendorf and M. Fendorf

Clays and Clay Minerals 44 220-227 *1996*

The retention of hazardous species, including many of the lanthanides, on soils and sediments is vital for maintaining environmental quality. In this study, high-resolution transmission electron microscopy (HRTEM) was used to identify surface precipitates of La and their degree of atomic ordering on oxides of Mn (birnessite), Fe (goethite), and Ti (rutile) over a pH range of 3 to 8. At pH >5.5, the aqueous concentration of La was fully depleted by all three metal oxides. On birnessite, surface precipitation of La-hydroxide occurred at pH $\geq$5 and appears to be the dominant sorption mechanism on this mineral. Surface precipitation was not observed on rutile or goethite until much higher pH values, 6.5 for rutile and 8.0 for goethite. Precipitation is thus correlated with the points of zero charge (PZC) of the minerals (6.3 and 7.8 respectively), and in each case was observed only at pH values above the PZC. Although La sorption was extensive on all the minerals at the higher pHs, the depletion of La from solution by rutile and goethite at pH values well below the PZC indicates that the sorption mechanism differs from that on birnessite, surface complexation of monomeric or small multi-nuclear species appears to predominate for La retention on rutile and goethite at most commonly encountered pH values.

38465 □ **Electron Microscopy of Thin Films Prepared by Laser Ablation**

H. Lemke, C. Echer and G. Thomas

IEEE Trans. Magn. 32 *1996*

A simple processing model has been developed for studying Nd-Fe-B magnets. The grain structure of these samples is comparable to that of melt-spun magnets. The samples are prepared by depositing films on a carbon foil TEM grid by laser ablation. The influence of temperature on the grain structure is emphasized. Deposition at room temperature yields amorphous films. Crystallinity is obtained at heater temperatures above 600°C during deposition. The size of the grains is about 20nm.

no # ■ **Ultrafast Response of As-Implanted GaAs Photoconductors**

H.H. Wang, P. Grenier, J.F. Whitaker, H. Fujioka, J. Jasinski, and Z. Liliental-Weber

IEEE-J. Sel. Topics *(in press)*

The photoconductive response of an optoelectronic switch fabricated from GaAs implanted with arsenic ions is measured to have a duration as short as 0.7 ps and a relaxation time as fast as 0.5 ps. The switching efficiency and relaxation time of the photoswitches using the As-implanted GaAs substrates are determined to be comparable to photoconductive devices employing GaAs grown by low-temperature molecular-beam epitaxy (LT-GaAs). For high dc-bias values, persistent photocurrent tails from transient leakage currents are found to be very prominent in bulk GaAs devices that were implanted with 10^{16} cm^{-2} arsenic ions at 200keV. This behavior has been determined to arise from substrate leakage current underneath the thin implanted layer, which recrystallizes and exhibits, as does LT-GaAs, arsenic-precipitate formation after annealing. In order to reduce this leakage current, multiple ion dosages with various implantation energies have been implemented. An epitaxial GaAs layer has also been implanted with arsenic ions, isolated from its semi-insulating substrate, and bonded onto a fused silica wafer in order to verify that the persistent tail response from the photoconductive switches was not actually due to the implanted region of GaAs.

38255 **Structure and Morphology of Nanosized Lead Inclusions in Aluminum Grain Boundaries**

E. Johnson, S. Hinderberger, S.-Q. Xiao, U. Dahmen and A. Johansen

Interface Science 3 279-288 *1996*

Grain boundary lead inclusions formed by ion implantation of mazed bicrystal aluminum films have been investigated by transmission electron microscopy. The vapor-grown bicrystal films contained mainly 90° <110> tilt boundaries with fixed misorientation but variable inclination, as well as some growth twins with 70.5° <110> symmetrical tilt boundaries and a few small-angle boundaries. It was found that the shape, size and orientation of the inclusions in the grain boundaries depend on the orientation of the aluminum grain boundary plane. Inclusions at 90° <110> tilt boundaries were invariably sharply faceted toward one aluminum grain and *more* rounded toward the other grain. The faceted side was a section of the cuboctahedral equilibrium shape of bulk lead inclusions in parallel topotaxy with the aluminum matrix. The rounded side, where the aluminum grain was rotated by 90° with respect to the lead lattice, approximated a spherical cap. At specific low-energy segments of the grain boundary where a (100) plane in grain 1 meets an (011) plane in grain 2, only two of several possible shapes were observed. One of these was preferred in as-implanted samples while both types were found after melting and re-solidification of the lead inclusions. The observations are discussed in terms of a modified Wulff construction.

No. # ■ **Influence of the Growth Mechanism on the Grain Boundary of Structure in $YBa_2Cu_3O_7$**

J. Ayache, A. Thorel, J. Le Duigou, J. Bonevich and U. Dahmen

J. Alloys and Compounds *(in press)* 1996

The growth control of thin $YBa_2Cu_3O_7$ film bicrystals determines the quality of Josephson junctions and weak links. Previous TEM experiments on various thin film bicrystals showed grain boundary oscillations that were not clearly explained. We combined AFM, SEM, conventional TEM and HRTEM in order to perform a complete characterization of both substrate and $YBa_2Cu_3O_7$ thin film bicrystals. Our results clearly show that the grain boundary oscillations are due to the YBCO growth mechanisms leading to a conflictual crystallographic situation at the grain boundary. The resulting crystallographic structure of the grain boundary may affect the interpretation of several recent experiments purporting to determine the nature of HTC superconductivity.

38300 ■ **Zirconium Nitride Precipitation in Nominally Pure Yttria-Stabilized Zirconia**

D. Gómez-García, J. Martínez-Fernández, A. Domínguez-Rodríguez and K.H. Westmacott

J. Am. Ceram. Soc. 79 487-490 *1996*

Nominally pure yttria-stabilized zirconia alloys are shown to contain unsuspectedly large amounts of dissolved nitrogen. Its presence in the lattice was detected through the observation of large precipitates in alloys with three different concentrations of yttria deformed in compression in argon in the temperature range 1600-1800°C. Electron diffraction, EDS and PEELS analyses and Moiré imaging were used to identify the precipitates as ZrN. The possible origin of the nitrogen, its likely effects on properties and the role of annealing atmosphere are briefly discussed.

38301 ■ **Electron-Beam-Induced Loop Formation on Dislocations in Yttria Fully-Stabilized Zirconia**

D. Gómez-García, J. Martínez-Fernández, A. Domínguez-Rodríguez and K.H. Westmacott

J. Am. Ceram. Soc. 79 2733-38 *1996*

The nature of the strain lobes and loops that form on edge-dislocations in yttria stabilized zirconia during exposure in an electron microscope has been investigated. By changing the operating conditions, such as acceleration voltage, cycling the beam intensity, heating or cooling the specimen prior to observation, or heat treatment prior to the deformation, it has been shown that the effects result from beam heating. During specimen heating ZrN precipitates which have a large misfit with the ZrO_2-Y_2O_3 matrix form in the compressed regions of the dislocation core.

37569 **Polymeric Sol-Gel Synthesis of $La_{1-x}Sr_xMnO_3$ Thin Films Exhibiting Giant Magnetoresistance**

A. Modak and K.M. Krishnan

J. Am. Ceram. Soc. *(submitted)*

We report here, for the first time, a reproducible polymeric sol-gel process for the synthesis of $La_{1-x}Sr_xMnO_3$ thin films exhibiting giant magnetoresistance. We have utilized a combination of metal alkoxide, β-diketonate and carboxylate compounds to form the complex precursor which underwent further processing steps of hydrolysis, spin coating and heat treatment. Key features of the process are its overall simplicity, low processing temperature, ease of composition variation, and ability to produce a wide range of structures. The underlying precursor chemistry, leading to atomic scale mixing of elements that occupy the same crystallographic site, critical to the successful synthesis of these films, has also been established. Single phase LSMO(80/20) thin films with a cubic structure (a = 0.38nm) were obtained and confirmed by x-ray diffraction and transmission electron microscopy observations. Epitaxy with (100) normal orientation was induced by deposition on $LaAlO_3$(100) substrates, while polycrystalline thin films were obtained on Si(100) substrates. Magnetoresistance properties comparable to or better than those of films of similar composition obtained by other techniques were observed, further corroborating the feasibility of the process.

38885 ■ **Indentation and Oxidation Studies on Silicon Nitride Joints**

M. Gopal, L.C. De Jonghe, G. Thomas

J. Am. Ceram. Soc. *(submitted)* 1996

Silicon nitride (Si3N4) ceramics have been joined with a yttrium oxide-silicon dioxide interlayer. A 1:2 molar ratio of Y2O3 to SiO2 was chosen to obtain the desired Y2Si2O7 stoichiometry, which should give the interlayer better oxidation resistance compared to other interlayer materials. Mechanical characterization of the joints performed by indentation shows it to have good room temperature strength.

37367 ■ **Epitaxial $Fe_{16}N_2$ Films Grown on Si(100) by Reactive Sputtering**

M.A. Brewer, K.M. Krishnan and C. Ortiz

J. Appl. Phys. 79 5321-53 *1996*

We present a crystallographic template for the growth of the range of Fe-N phases on Si(001) by lattice matching on selected underlayers. Epitaxial films of pure a-Fe, g-Fe_4N and a'-Fe_8N (N martensite) were grown individually by the optimization of reactive N_2 sputtering parameters. The orientation relation of the Fe-N phases was Fe-N(001) || Ag(001) || Si(001) and Fe-N[100] || Ag[110] || Si[100]. Annealing the a'Fe_8N films resulted in the formation of a'-Fe_8N/a"-$Fe_{16}N_2$ mixtures. In addition to the crystallographic and structural analysis, quantification of x-ray diffraction peak intensities confirmed that the a'/a" mixtures contained as much as 46 vol% a" (remaining a'). VSM and SQUID magnetometry measurements of the a' and a'(54%)/a"(46%) mixture, respectively, indicate enhanced magnetic moments for both the a' and a" phases with respect to pure Fe.

37368 ■ **Role of Epitaxy and Polycrystallinity in the Magnetoresistance and Magnetization of La0.8Sr0.2MnO3 Thin Films**

K.M. Krishnan, A.R. Modak, C.A. Lucas, H.B. Cherry and R. Michel

J. Appl. Phys. 79 5169-51 *1996*

Alkaline earth substituted manganese oxides, $La_{1-x}A_xMnO_3$ (A = Ca, Sr, or Ba), with perovskite structures, have attracted much recent attention because of their very large magnetoresistance for composition in the range $0.1 < x < 0.4$. However, the fundamental mechanism governing their galvanomagnetic properties and magnetization behavior, is, as yet, not understood. Moreover, these properties are observed to be dependent on conditions of growth and annealing, composition, oxidation state, epitaxy and the overall microstructure. More detailed characterization of the structure and properties of these films and the epitaxial growth of similar films with well defined grain boundaries is in progress.

37366 ■ **Microstructure and Composition in Rapidly Quenched NdFeB-Based Hard Magnet Alloys**

T.D. Nguyen, K.M. Krishnan, L.H. Lewis, Y. Zhu and D.O. Welch

J. Appl. Phys. 79 4848-48 *1996*

A detailed comprehension of the microstructure and composition in NdFeB hard magnet alloys is important in understanding their magnetic properties and reversal mechanisms. In this study, transmission electron microscopy (TEM) studies of the grain boundary phases in melt-quenched, thermomechanically-processed magnet alloys based on the $Nd_2Fe_{14}B$ composition, utilizing high resolution, analytical, and Lorentz techniques, are presented. The relationship between the observed microstructure and magnetic properties, and in particular the reversal mechanism in these materials are discussed.

37722 ■ **Plasma Distribution of Cathodic Arc Deposition Systems**

S. Anders, S, Raoux, K. Krishnan, R.A. MacGill and I.G. Brown

J. Appl. Phys. 79 6785-67 *1996*

The plasma distribution using a cathodic arc plasma source with and without magnetic macroparticle filter has been determined by depositing on a transparent plastic substrate and measuring the film absorption. It was found that the width of the distribution depends on the arc current, and it also depends on the cathode material which leads to a spatial separation of the elements when an alloy cathode is used. By applying a magnetic multicusp field near the exit of the magnetic filter, it was possible to modify the plasma distribution and obtain a flat plasma profile with a constant and homogeneous elemental distribution which was demonstrated by depositing FeNd thin films.

38557 ■ **The Effect of Excess Gallium Vacancies in Low-temperature GaAs/AlAs/GaAs: Si Heterostructures**

C. Kisielowski, A.R. Calawa, Z. Liliental-Weber

J. Appl. Phys. 80 156-160 *1996*

This article shows that the presence of low-temperature-grown GaAs (LT-GaAs) LT-GaAs/AlAs/GaAs:Si heterostructures increases the Al/Ga interdiffusion at the heterostructure interfaces. The interdiffusion enhancement is attributed to the presence of Ga vacancies (V_{Ga}) in the As-rich LT-GaAs, which diffuses from a supersaturation of V_{Ga} frozen-in during sample growth. Chemical mapping, which distinguishes between the AlAs and GaAs lattices at an atomic scale, is used to measure the Al concentration gradient in adjacent GaAs:Si layers. A correlation is observed between the Al/Ga interdiffusion and the gate breakdown voltage in metal-insulator field-effect transistor structures containing LT-GaAs.

no # ■ **Homoepitaxial Growth of GaN Using Molecular Beam Epitaxy**

A. Gassmann, T. Suski, N. Newman, C. Kiselowski, E. Jones, E.R. Weber, Z. Liliental-Weber, M.D. Rubin, H.I. Helava, et. al.

J. Appl. Phys. 80 1342 *1996*

In this paper, experimental results are presented for the first homoepitaxial deposition of a GaN overlayer onto a bulk single-crystal GaN substrate using Molecular Beam Epitaxy. Transmission electron microscopy shows a superior structural quality of the deposited GaN overlayer when compared to heteroepitaxially grown layers. Photoluminescence shows narrow excitonic emission (3.467 eV) and very weak yellow luminescence, whereas the bulk substrate luminescence is dominated by this deep level emission. These results show that homoepitaxy of GaN can be used to establish benchmark values for the optoelectronic properties of GaN thin films.

---

no # ■ **Microstructure of Thin GaN Layers grown on (001) GaAs by Plasma-assisted Molecular-beam Epitaxy**

S. Ruvimov, A. Liliental-Weber, J. Washburn

J. Appl. Phys. *(in press)*

High resolution electron microscopy has been applied to characterize the structure of β-GaN epilayers grown on (001) GaAs substrates by plasma-assisted molecular-beam-epitaxy. An rf plasma source was used to promote chemically active nitrogen. An As flux was applied during the growth of the first few monolayers to control the nucleation process. The best quality GaN layers with abrupt interfaces were achieved by near-stoichiometric nucleation with optimal Ga to N ration. Deviation from these nucleation conditions leads to interface roughening and formation of the wurtzite phase within the GaN layer probably due to different properties of α compared toβ dislocations in cubic GaN. The majority of stacking faults intersect the interface along lines parallel to the major flat of the GaAs wafer. The stacking faults are often associated with atomic steps at the GaN-GaAs interface.

No. # □ **Change of Structure and Location of Misfit Dislocations in $In_xGa_{1-x}As/GaAs$ (001) System**

Y. Chen, H. Sohn, Z. Liliental-Weber, J. Washburn, J.F. Klem and J.Y. Tsao

J. Appl. Phys. *(submitted)*

The structure and locations of misfit dislocations have been investigated experimentally and theoretically in different strained $In_xGa_{1-x}As$ ($0.2 \leq x \leq 1$) epilayers grown on GaAs substrates. The misfit dislocations in the $In_{0.2}Ga_{0.8}As$ epilayers were predominantly dissociated 60° dislocations with the 90° partials lying in the interface and the 30° partials pushed into the substrate. In $In_{0.3}Ga_{0.7}As$ epilayers, misfit dislocations of both 60° and 90° types were present either in undissociated form or split into partials. These dislocations were not all near the interface; some were scattered through the epilayer. The presence of dislocations of 60° type located away from the interface for intermediate misfits is rationalized by considering the balance of forces acting on these dislocations. In $In_{0.4}Ga_{0.6}As$ and in InAs epilayers, misfit strain was accommodated almost entirely by 90° undissociated dislocations. A model is proposed for the formation of 90° edge dislocations to explain the transition of dominant misfit dislocation type from 60° to 90° type with increasing mismatch.

39353 □ **Magnetic and Physical Microstructure of $Fe_{16}N_2$ Films Grown Epitaxially on Si(001)**

M.A. Brewer, C.J. Echer, K.M. Krishnan, T. Kobayashi and A. Nakanishi

J. Appl. Phys. *(submitted)* 1996

Epitaxial $Fe_{16}N_2$ films were grown on Si(001) substrates with a Ag underlayer by reactive sputtering in nitrogen. Pure α'-Fe_8N films were obtained which on subsequent annealing resulted in mixtures of (54%) and a''-$Fe_{16}N_2$ (46%). An average moment of 1780 emu/cc, considerably larger than that of pure α-Fe (1714 emu/cc), was measured for both samples. Plan-view transmission electron microscopy (TEM) of the films confirms the orientation relationship $Fe_{16}N_2$ (001) ø Ag(001) ø Si[100], and a small grain size (~100 Å), while EELS analysis confirms an average composition of Fe_8N for both samples. Electron diffraction patterns indicate that the as-deposited α1 films already contain very small regions of ordered α'' which were not previously detected by XRD measurements. Mössbauer spectroscopy performed at both 300K and 16K gave three hyperfine fields corresponding to three different iron sites for both the unannealed α' and the annealed α'/ α'' mixtures. Lorentzian fitting of the three iron components for the α'/ α'' spectrum obtained at room temperature gave an intensity ratio of 1:2:1 (FeI:FeII:FeIII) corresponding to the expected occupancy for the three Fe sites in the $Fe_{16}N_2$ structure.

no # ■ **Structural, Electrical and Optical Studies of GaAs Implanted with MeV As or GaIons**

J. Jasinski, Z. Liliental-Weber, J.Washburn, H.H.Tan, C. Jagadish, et. al

J. Elec. Materials *(in press)* 1997

Structural properties of GaAs implanted with high doses of 2 MeV arsenic or gallium ions with annealing at different temperatures were studied by TEM, Rutherford backscattering spectrometry-channeling double crystal x-ray diffraction. Optical absorption, electrical conductivity, Hall-effect and time-resolved photoluminescence were applied to monitor changes in electrical and optical characteristics of material. A conclusion from this investigation is that there is hardly any difference between materials implanted with gallium or arsenic. For implantation of either species, a large number of point defects were introduced and for a high enough dose a buried amorphous layer was formed. Hopping conduction and high absorption below band-to-band transition were observed for both cases. After low temperature annealing of amorphous material a high density of stacking faults and microtwins were found. Regrowth rates at the front and back amorphous-crystalline interfaces showed a significant difference. This was attributed to differences in local non-stoichiometry of material at upper and lower amorphous-crystalline interfaces.

---

no # ■ **Structural Characterization of Bulk GaN Crystals Grown Under High Hydrostatic Pressure**

Z. Liliental-Weber, C. Kisielowski, S. Ruvimov, Y. Chen, J. Washburn, I. Grzegory, M. Bockowski, J. Jun, and S. Porowski

J. Elect. Materials 25 1545-50 *1996*

This paper describes TEM characterization of bulk GaN crystals grown at 1500-1800K in the form of plates from a solution of atomic nitrogen in liquid gallium under high nitrogen pressure (up to 20 kbars). The x-ray rocking curves for these crystals were in the range of 20-30 arc-sec. The plate thickness along the c axis was about 100 times smaller than the nonpolar growth directions. A substantial difference in material quality was observed on the opposite sides of the plates normal to the c direction. On one side the surface was atomically flat, while on the other side the surface was rough, with pyramidal features up to 100 nm high. The polarity of the crystals was determined using convergent-beam electron diffraction. The results showed that, regarding the long bond between Ga and N along the c-axis, Ga atoms were found to be closer to the flat side of the crystal, while N atoms were found to be closer to the rough side. Near the rough side, within 1/10 to 1/4 of the plate thickness, there was a high density of planar defects (stacking faults and dislocation loops decorated by Ga/void precipitates). A model explaining the defect formation is proposed.

37599 ■ **Electron Microscopy and Microanalysis of Ceramics**

G. Thomas

J. European Ceram. Soc. 16 323-338 *1996*

We live and work in a world that depends on materials and their performance. The science of materials has developed to a position of great understanding, such that materials can be microscopically tailored to provide specific sets of properties. The practical applications of newly designed materials depend on market interest and costs. In the final analysis it is the processing of materials that remains the key factor. In order to facilitate technical advances, the relationships between processing, microstructure, and performance must be established. This task is generic to all materials whether for mechanical or physical property goals. Central to such understanding is the role played by electron optical, diffraction and analytical methods of characterization in their specificity to synthesis to the atomic level. This paper provides some examples of such applications to several ceramic systems, and attempts to indicate the generic nature of many problems to be solved.

no # ■ **Mullite-Aluminosilicate Glassy Matrix Substrates Obtained by Reactive Coating**

J. Requena, J.R. Bartolome, J.S. Moya, S. De Aza, F. Guitian, G.Thomas

J. European Ceram. Soc. 16 249-254 *1996*

Layered kaolinite-alumina composites have been obtained by a sequential slip casting technique. The interfacial reaction as well as the microstructure of different layers have been studied in laminates fired at 1650°C. The results are discussed on the basis of the SiO_2-Al_2O_3-K_2O equilibrium diagram. Taking into account these results, a new lost cost ceramic substrate for electronic applications--reinforced by mullite whiskers and with controlled closed porosity, low permittivity value ($\varepsilon \approx 4$ at 1 MHz) and thermal expansion coefficient close to that of silicon ($3{\cdot}8 \times 10^{-6}\ °C^{-1}$) - has been developed starting from conventional kaolinite powder.

no # **Electron Microscopy of Giant Magnetoresistive Granular Au-Co Alloys**

J. Bernardi, A. Hutten, G. Thomas

J. Mag. Mat. 157/158 153-155 *1996*

The microstructure and the magnetic properties of melt-spun $Au_{100-x}Co_x$ (x=6.5, 16.7, 28.4) were investigated. The eutectic decomposition allows one to synthesize a lamellar microstructure. Changes of the size distribution and shape of the Co precipitates during annealing influence the magnetic behavior and the transport properties of the investigated samples.

No. # ■ **Investigations of the Compositional Distribution in Epitaxially Grown Co-Cr Thin Films with Enhanced Saturation Magnetisation**

D.J. Rogers, T. Maeda and K.M. Krishnan

J. Mag. Mat. 163 393-396 *1997*

The compositional distribution in a $Co_{78}Cr_{22}$ film grown epitaxially on Ru/mica by electron beam evaporation was investigated using spin-echo ^{59}Co nuclear magnetic resonance (NMR) and preferential chemical etching of Co. NMR revealed evidence for the occurrence of drastic compositional separation producing a Co-enriched component containing almost pure Co. Chemical etching revealed a particularly fine distribution of Co-enriched regions. These results are consistent with the proposition that the enhanced saturation magnetisation (M_s) observed in these films is attributable to enhanced compositional inhomogeneities.

Keywords: Co-Cr film; Compositional separation; Magnetic recording; Nuclear magnetic resonance; Chemical etching

---

39287 ■ **Effect of TiO_2 Doping on Rapid Densification of Alumina by Plasma Activated Sintering**

R.S. Mishra, A.K. Mukherjee, K. Yamazaki and K. Shoda

J. Mat. Res. *(in press)*

The effects of plasma cycle and TiO_2 doping on sintering kinetics during plasma activated sintering (PAS) of g-Al_2O_3 have been studied in the temperature range of 1473-1823 K. Multiple plasma cycle leads to higher densification. Also, TiO_2 doping enhances the sintering kinetics during PAS. In TiO_2 doped specimens, near full density was obtained at 1673 K in less than 6 minutes using multiple plasma cycle. It is suggested that the dielectric properties of a material are critical for the success of the PAS process.

39166 ■ **Phase Behavior of Ordered Diblock Copolymer Blends: Effect of Compositional Heterogeneity**

R.J. Spontak, J.C. Fung, M.B. Braunfeld, J.W. Sedat, D.A. Agard, L.Kane, S.D. Smith, M.M. Satkowski, A.Ashraf, D.A. Hajduk and S.M.

Macromolecules 29 4494-45 *1996*

Diblock copolymers order into a variety of periodic morphologies when c N > (c N) $_{ODT,}$ where c is the Flory-Huggins interaction parameter, N is the number of statistical segments, and ODT denotes the order-disorder transition. Previous studies have demonstrated that classical dispersion (spherical and cylindrical) and lamellar morphologies, as well as novel complex morphologies (*e.g.*, gyroid*, lamellar catenoid, and hexagonally perforated lamellae), can be selectively accessed through either tailored molecular synthesis or copolymer/homopolymer blends. In the present work, control over ultimate morphology is achieved through the use of binary copolymer blends composed of two strongly-segregated poly (styrene-*b* -isoprene) (SI) diblock copolymers of comparable N but different compositions. Blend morphologies are examined by electron microscopy (including 3-dimensional imaging) and small-angle x-ray scattering, and a theoretical framework is proposed to describe strongly-segregated blends exhibiting the lamellar morphology. Results obtained indicate that diblock copolymer blends behave as neat diblock copolymers of equal bulk composition, suggesting that such blends offer an alternative, and attractive, route by which to generate a desired morphology.

37752 ■ **Applications of Electron Microscopy to Industrial Research**

F.M. Ross, K.M. Krishnan, N. Thangaraj, R.F.C. Farrow, R.F. Marks, A. Cebollada, S.S.P. Parkin, et al

MRS Bulletin 21 17-23 *1996*

The transmission electron microscope (TEM) is one of the most successful tools available to the materials scientist. Yet both the complexity and expense of the equipment, and the huge investment in time necessary to become proficient in specimen preparation and image acquisition and analysis, mean that it is difficult for most industrial institutions to maintain a state-of-the-art TEM facility. How can industry overcome this problem? One solution is to set up a collaboration with a university, an industrial partner or a government research laboratory. Such a collaboration can be extremely valuable to the company, which gains access to microscopes, specimen preparation equipment and the expertise of professional microscopists, and to the research laboratory, which benefits from the industrial perspective and the private sector's proficiency in materials preparation and processing. In this paper we present three case studies of successful collaboration between industry and the National Center for Electron Microscopy.

---

no # ■ **HRTEM Studies of Two New (Nd, Ca)$_x$ W0$_3$ Bronzes Synthesized under High Pressure Conditions**

N. D. Zaharov, Z. Liliental-Weber, V.P. Filonenko, I.P. Zibrov and M. Sundberg

MRS Bulletin 21 373-380 *1996*

Two new (Nd, Ca)x W0$_3$ bronzes have been prepared by solid state reaction at P= 50 kbar and T = 1520 K. The compounds were studied by X-ray powder diffraction and high resolution transmission electron microscopy. One phase was identified to be of hexagonal tungsten bronze type, while the other one was found to have the intergrowth tungsten bronze structure (2)-ITB. Disorder in terms of varying widths of the HTB and W0$_3$ slabs was sometimes observed. HTB tunnel rows terminating in the (2)-ITB structure were also seen. The neodymium and calcium contents in the two phases were confirmed by EDS analysis.

37600 ■ GMR Behavior of Nanostructured Heterogeneous M-Co (M=Cu, Ag, Au) Alloys

J. Bernardi, A. Hutten, G. Thomas

Nanostructured Materials 7 205-220 *1996*

Heterogeneous M-Co (M=Cu, Ag, Au) Alloys have been observed by transmission electron microscopy (TEM). The magnetic properties and the GMR effect are compared with the evolution of the microstructure after preparation of the samples and after annealing. Limiting effects in TEM that prevent resolving ferromagnetic Co precipitates in Cu-Co-or AG-Co can be overcome by choosing the System Au-Co. Annealing causes a coarsening of the Co precipitates and an increase in the interparticle distance. Lorentz microscopy confirms single domain Co particles exist in as-quenched $Au_{71.6}Co_{28.4}$ ribbons, and multidomain Co particles in annealed ribbons, respectively. The changes in the grain size and the formation of multidomain particles can be exactly correlated with magnetic measurements.

39964 ■ TEM Study of Nanocrystalline NdFeB

M.V. P. Altoe, C.E., Echer, G. Thomas

Nanostructured Materials *(in press)* *1996*

A detailed study is reported of the microstructure in a nanocrystalline alloy, $Nd_4Fe_{78}B_{18}$, consisting of a mixture of hard($Nd_2Fe_{14}B$) and soft (Fe_3B) magnetic phases, utilizing conventional and analytical transmission electron microscopy (TEM). The nanocrystalline microstructures were fabricated by annealing the melt-spun amorphous $Nd_4Fe_{78}B_{18}$ ribbons by means of conventional (furnace) annealing techniques and also by the so-called flash-annealing process. Enhanced remanence and coercivity were reported previously for the flash-annealed alloys. Furnace-annealed ribbons contained 20-30 nm equiaxed grains with Fe/Nd =17 - 19.6. Also observed were large (50-100 nm) equiaxed grains of[alpha]-Fe. For flash-annealed ribbons, significant amounts of $Nd_2Fe_{23}B_3$,a metastable cubic phase, were observed, as well as a marked difference in the second phase morphology. For the flash-annealed ribbon whose hysteresis loop showed good coupling of the magnetic phases, a refined microstructure was found and the large [alpha]-Fe grains were absent.

39186 ■ Characterization of Nano-magnetic Structures

G.Thomas, A. Hutten

Nanostructured Materials *(in press)* *1996*

Since many important magnetic properties are affected (and thus can be manipulated) by microstructural features, it is important to characterize the physical and magnetic structures at the highest resolutions. Unfortunately, the resolution of electron microscopes is optimized for a given wavelength by high field lenses (~1-2 tesla), which can easily saturate the specimen. Thus, to obtain high resolution structural and magnetic information in the same instrument is not possible, unless it is specially designed or sufficiently flexible. An example of the latter is the improved magnetic resolution obtained on the 800 kV Berkeley ARM and its applications to domains in Co-X binary alloys. Much of the restriction on high resolution revolves around specimens very thin in the beam direction (* 200 Å) and the signal-to-noise problem. Even with high resolution, sufficient image contrast is necessary to define the mesostructure. This paper discusses some of these issues, together with the problem of identification of atomic species, and effects associated with interfaces. Examples are drawn from current work on hard magnets, oxides and GMR in alloys.

39187 ■ Magnetic Properties of Nd-Fe-B Films Analyzed by Lorentz Microscopy

H. Lemke, G. Thomas, D. L. Medlin

Nanostructured Materials *(in press)*

A *JEOL4000EX* microscope operated in the Lorentz mode was used to analyze the magnetic structure in pulsed laser deposited films. The films consist of grains of 20 nm with $ND_2Fe_{14}B$ as the hard magnetic phase. The thickness of the grain boundary is between 1 and 2 nm. Most domains follow the grain boundaries, some, however, seem to intrude the grains. The influence of film thickness on the magnetic properties is emphasized. An increase of film thickness from 100 nm to 200 nm leads to a decrease in domain size from 500 nm to 100 nm, while the crystalline properties remain the same.

39500 ■ TEM and RBS/Channeling of Nanosized Bicrystalline (Pb,Cd) Inclusions in Al Made by Sequential Ion Implantation

E. Johnson, V.S. Tuboltsev, A. Johansen, U. Dahmen and S. Hagege

Nuc. Instr. & Methods in Phys. Res. *(in press) 1996*

Sequential ion implantation of Pb and Cd in Al at 425 K and 475 K respectively has been used to produce dense distributions of nanosized (Pb,Cd) inclusions with equiatomic composition. Pb and Cd form a simple eutectic system, but both elements are insoluble in solid Al, and the inclusions are Cd-rich in comparison with the eutectic composition. Inclusions in the size range from 1 to 20 nm were observed in as-implanted samples. Their overall shape was nearly cuboctahedral. Most of the inclusions were bicrystalline with an fcc Pb part forming a segment of a cuboctahedron and an hcp Cd slab attached to one of the $\{111\}_{Pb}$ facets. The orientation relationship had close-packed planes and directions parallel in the three structures. In-situ melting/solidification experiments combining TEM and RBS/channeling showed that melting of the inclusion ensemble occurs within a narrow temperature interval of 10 - 15 K around the eutectic temperature of 521 K. Solidification takes place with undercoolings of about 50 - 65 K below the liquidus line in a two-stage process where Cd solidifies 15 to 20 K before Pb.

37595 ■ The Effect of Twinning on the Shapes of Cube-Cube-Related Ge Precipitates in Al

S.Q. Xiao, S. Hinderberger, K.H. Westmacott and U. Dahmen

Phil. Mag. A 73 1261-78 *1996*

This work establishes a correlation between the shape and internal twin structure of cube-cube related Ge precipitates in Al. Using conventional and high resolution electron microscopy, it is shown that most triangular plates have only one twin variant, parallel to the habit plane. Hexagonal plates have two or more twins of the same variant, parallel to the habit plane. Most tetrahedral precipitates have two non-coplanar twin variants. Small octahedral precipitates are twin-free, while larger octahedra can have up to 2 twin variants. The different shapes are due to preferential growth at grooves formed by reentrant twin junctions, and an increased mobility of the interfaces between the matrix and a twinned precipitate. It is shown that precipitates nucleate as twin-free octahedra. The effect of single, double and secondary twinning on precipitate growth is analyzed systematically, and compared with experimental observations. Symmetry considerations show that all three precipitate forms are consistent with Curie's principle if the de-symmetrizing effect of twinning is taken into consideration.

38097 ■ Transmission Electron Microscopy of the AlN-SiC Interface

F.A. Ponce, M.A. O'Keefe and E.C. Nelson

Phil. Mag. A 74 777-789 *1996*

The AlN/SiC interface has been studied using high resolution transmission electron microscopy. Cross section lattice images of the AlN/SiC interface have been analyzed to establish the connection between image contrast and the atomic positions in the lattice. Assuming atomically abrupt and planar AlN/SiC interfaces, four possible atomic bonding configurations are taken into account for SiC substrates with the (0001)Si orientation. Image simulations of these four interface models are compared with the experimental images. Considering variations at the interface of the image contrast, the basal-plane distance, and the projected charge density, it is shown that the C-Al and Si-N bonds are in agreement with the experimental images and are not distinguishable under our experimental conditions. The other two possibilities, involving C-N and Si-Al bonds, are not consistent with our observations.

38257 ■ Phase Transformation of TiO_2 Precipitates in Sapphire Induced by the Loss of Coherency

S.Q. Xiao, U. Dahmen and A.H. Heuer

Phil. Mag. A 75 221-238 *1997*

The first phase to precipitate in Ti-doped sapphire ($a\text{-}Al_2O_3$) single crystals annealed at 1300°C in air is a high pressure form of titanium dioxide with the a-PbO2 structure ($a\text{-}TiO_2$). The precipitates form as oblate spheroidal plates with habit planes parallel to $(0001)_s$. Because the $a\text{-}TiO_2$ precipitates are coherent with the sapphire matrix when small, they are under compressive stress resulting from a 5% lattice mismatch with sapphire. During coarsening they lose coherency by emitting a dislocation loop with a 1/3<1101>s Burgers vector. The loss of coherency reduces the stress on the precipitates, and allows them to transform to the rutile structure. The orientation relationship between the sapphire matrix, $a\text{-}TiO_2$ and rutile has been determined and a lattice correspondence for the phase transformation proposed. Although the transformation from $a\text{-}TiO_2$ to rutile is purely structural, its rate is controlled by diffusion because the increased atomic volume of rutile is accommodated by expelling extra mass into the nearby dislocation loop, and is associated with a change in the precipitate shape.

37723 ■ Crystallographic Aspects of Pore Formation in GaAs

F.M. Ross, G. Oskam, P.C. Searson, J.M. Macaulay and J.A. Liddle

Phil. Mag. A *(in press) 1996*

The structure of porous layers formed in n-type gallium arsenide is characterized and compared with the more familiar structure of porous n-type silicon formed under analogous conditions. Although similar in many respects, the pores formed show characteristic differences which provide insight into the pore formation process. The morphology is discussed in terms of a simple model in which we consider the bonding configuration of atoms on steps, kinks and terraces on the interior of the pore and the spatial distribution of the rate-limiting electrochemical reactions.

38372 ■ Morphology, Structure and Thermal Behavior of Small Eutectic Pb-Cd Inclusions in Aluminum

S. Hagège and U. Dahmen

Phil. Mag. Lett. 74 259-266 *1996*

Small inclusion of eutectic Pb-Cd embedded in a solid Al matrix were produced by melt spinning and investigated by transmission electron microscopy. Inclusions were found to be phase separated into two parts, one face-centered cubic and Pb-rich, the other hexagonal close-packed and Cd-rich. The two phases maintained an orientation relationship of parallel close-packed planes and directions with each other and with the fcc Al matrix. The inclusion shape was anisotropic and each segment displayed the facets typical for pure Pb and pure Cd inclusions found in binary Al-Pb and Al-Cd alloys. Within the observed size range of 5 to 100 nm, particles exhibited a single Pb-Cd interface, invariably parallel to the shared close-packed plane. The bimetal inclusions were found to melt at the eutectic bulk melting point regardless of size. Melting was initiated at the triple interface junction of Cd, Pb and Al. By comparison, solidification during cooling required an undercooling of about 35°C and took place very rapidly in less than 1/30 s. The volume change during solidification led to an elastic distortion of the surrounding matrix which subsequently decayed over a period of over 20s.

39079 ■ Strain-related Phenomena in GaN Thin Films

C. Kisielowski, J. Kruger, S. Ruvimov, T. Suski, J. W. Ager III, E. Jones, Z. Liliental-Weber, et al

Phys. Rev. BII 54 17 745- *1996*

Photoluminescence (PL), Raman Spectroscopy, and x-ray diffraction are employed to demonstrate coexistence of a biaxial and a hydrostatic strain that can be present in GaN thin films. Biaxial strain originates from growth on lattice-mismatched substrates and post-growth cooling. An additional hydrostatic strain is shown to be introduced by presence of point defects. A consistent description of experimental results is derived within limits of linear and isotropic elastic theory using a Poisson ratio v=0.23±0.06 and a bulk modulus B=200±20 GPa. These isotropic elastic constants help judge validity of published anisotropic elastic constants that vary greatly. Calibration constants for strain-induced shifts of the near-band-edge PL lines with respect to E2 Raman mode are given for strain-free, biaxially strained, and hydrostatically contracted or expanded thin films.We determine that a biaxial stress of one GPa would shift the near-band-edge PL lines by 27 ±2meV and the E2 Raman mode by 4.2± 0.3 cm-1 by use of listed isotropic elastic constants. It is expected from the analyses that stoichiometric variations in the GaN thin films together with the design of specific buffer layers can be utilized to strain engineer material to an extent that exceeds possibilities known from other semiconductor systems because of different covalent radii of Ga and N atom.

39312 ■ Magic-Size Equilibrium Shapes of Nanosize Pb Inclusions in Al

U. Dahmen, S.-Q. Xiao, S. Paciornik, E. Johnson and A. Johansen

Phys. Rev. Lett. 78 471-474 *1997*

We show that the equilibrium shapes of small solid Pb inclusions embedded in an Al matrix are size dependent. Using high resolution electron microscopy we have observed that small inclusions a few nanometers in size adopt equilibrium shapes with smooth {111} facets. Inclusion dimensions follow preferred sizes shown to result from the nature of the residual strain which oscillates and decreases with size. As a result, the inclusion shape is controlled by the residual strain energy at small sizes and by the interface energy at larger sizes.

39667 ■ **Evidence for O_{2p} Hole Driven Conductivity in $La_{1-x}Sr_xMnO_3$ ($0 \le x \le 0.7$) and $La_{0.7}Sr_{0.3}MnO_z$**

H.L. Ju, H.C. Sohn, and K. M. Krishnan

Phys. Rev. Lett. *(in press)* 1997

Oxygen *K*-edge (core level excitation of oxygen 1*s* electrons into empty *p*-like states) electron energy loss spectra (EELS) have been measured for $La_{1-x}Sr_xMnO_3$ ($0 \le x 0.7$) and $La_{0.7}Sr_{0.3}MnO_z$ sol-gel derived thin films as a function of x and z. The spectra shows a prepeak at the Fermi level, corresponding to transitions to empty states in the O_{2p} band (oxygen 2p holes), at the threshold of the K-edge around 529eV. We have observed a remarkable correlation between the electrical resistivity and this prepeak intensity; i.e. the prepeak intensity increases with and increase in conductivity through systematic divalent doping (x) or oxygen stoichiometry (z) control. This confirms that the charge carriers in these manganese perovskites have significant oxygen 2p hole character and suggest that the "double exchange" mechanism has to be modified.

39286 ■ **Influence of Temperature on Segregation in 2009 Al-SiC_w Composite and Its Implication on High Strain Rate Superplasticity**

R.S. Mishra, C. Echer, C.C. Bampton, T.R. Bieler and A.K. Mukherjee

Scr. Met. et Mat. *(in press)* *1996*

The high strain rate superplasticity in 2009 Al-SiC_w composite is influenced by prior thermomechanical history. The influence of temperature on segregation in 2009 Al-SiC_w composite has been studied for the first time by in-situ transmission electron microscopy to establish the nature of segregation at high temperature. Contrary to some suggestions in the literature, in-situ analysis at room temperature and 500°C revealed that chemical inhomogeneity in the matrix and interfaces observed at room temperature disappear at 500 °C. The precipitates were observed to dissolve and the results agree well with the differential thermal analysis results. These results are also consistent with the theoretical expectation of dissolution of precipitates during heating above the solvus temperature. No elemental segregation was observed in this composite at room temperature. The implication of these results is that the mechanism of high strain rate superplasticity in aluminum alloy matrix composites is more likely to be microstructure related as compared to liquid phase assisted.

39280 ■ Structural Characterization of Bulk GaN Crystals

Z. Liliental-Weber, C. Kisielowski, X. Liu, L. Schloss, J. Washburn, E.R. Weber, I. Grzegory, M. Bockowski, J. Jun, T. Suski, et al

Sol. State Elec. *(in press) 1996*

TEM characterization of bulk GaN crystals grown at 1500-1800K in the form of plates from a solution of atomic nitrogen in liquid gallium under high nitrogen pressure (up to 20 kbars) is described. The plate thickness along the c axis was about 100 times smaller than along the nonpolar growth directions. A substantial difference in material quality was observed near the two opposite sides of the plates normal to the c direction. This was related to the polarity of the crystal. On one side the surface was almost atomically flat and the underlying material was free of any extended structural defects, while the other side was rough. The planar defects (dislocation loops and stacking faults formed on the basal planes) near the rough side of the crystal did not have a substantial influence on the FWHM of x-ray rocking curves. A large difference in crystal stoichiometry was observed in different sublayers of the crystals. Based on convergent beam electron diffraction and cathodoluminescence it was proposed that GaN antisite defects are related to the yellow luminescence observed in these crystals.

38402 ■ Cross-Sectional High Resolution Transmission Electron Microscopy of the Microstructure of Electrochromic Nickel Oxide

X.Y. Song, Y.X. He and C.M. Lampert

Solar En. Mat./Solar Cells *(submitted)* 1996

Electrochromic nickel oxide films on indium tin oxide (ITO) were investigated by cross section high resolution transmission electron microscopy and energy dispersive x-ray analysis. Microstructural features and the differences between high quality and poor quality samples were studied and compared. The dominant phase of the NiO film has cubic structure, but selected area electron diffraction patterns revealed many extra diffraction spots for the high performance samples which may result from additional hydrated nickel oxide phases. The NiO grains do not show clear shapes in the cross section plane nor are there signs of a preferred orientation. The mean grain size is larger and there are more defects and superlattices in samples with good electrochromic properties. There was a clear correlation between grain size distribution and performance. The high quality samples had a mean grain size of about 6.5nm, whereas the poor quality samples exhibited significantly smaller mean grain sizes of 5.0 and 3.8 nm.

37601 ■ **Dual Phase Steels Revisited: Reinforcement for Concrete**

G. Thomas

Trans. Indian Inst. Met. 49 127-132 *1996*

The utilization of dual-phase steel processing allows the design of composite microstructures whereby the advantages of the second phase are optimized, while the less desirable features of this phase are simultaneously mitigated by the presence of the other constituent phase. The size, morphology, distribution, shape and volume fraction of the second phase critically control the mechanical properties, especially fracture and fatigue, of such steel.s As a result, these structures offer a degree of metallurgical flexibility that is absent in conventionally processed alloys. Low carbon martensite/ferrite structures give high strength, cold formability, improved low temperature ductility, and improved corrosion resistance in concrete. This paper summarizes research results at U.C. Berkeley and redirects attention to low carbon dual-phase steels for applications to reinforcement of concrete. Their greatly improved corrosion resistance may permit the elimination of coatings with considerable potential for cost savings. These steels can be produced on line in a hot mill by controlled rolling and quenching.

36753 ■ **A Pattern Recognition Technique for the Analysis of Grain Boundary Structure by HREM**

S. Paciornik, R. Kilaas, J. Turner and U. Dahmen

Ultramicroscopy 62 15-27 *1996*

A pattern recognition technique for the detection of structural units in high resolution images of interfaces is described. The technique uses cross correlation functions as a means of locating atomic patterns characteristic for an interface and as a measure of similarity between related units. Application is not limited to periodic, or even to planar interfaces. Characteristic structural units can be extracted from an experimental image and some important parameters such as mirror or mirror glide symmetry, and rigid body displacements can be determined without knowledge of the imaging parameters. The technique allows an image of a structural unit with reduced specimen noise to be obtained by averaging over several similar units, even if a boundary is not periodic and not planar. Characteristic structural units so determined can subsequently serve as a basis for structure determination by a refinement process image simulation optimized for several experimental parameters.

39087 ■ **Deceptive "Lattice Spacings" in High-Resolution Micrographs of Metal Nanoparticles**

J.O. Malm and M.A. O'Keefe

Ultramicroscopy *(in press) 1996*

Experimental HRTEM images of randomly-oriented nanocrystals typically show fringes within the nanocrystals. Often these fringes are one-dimensional, although many appear to show two-dimensional resolution. In order to determine the tilt conditions necessary for the formation of one- and two-dimensional fringes in nanocrystals, simulations of HRTEM images of a 561-atom palladium nanoparticle were carried out over an extensive range of tilts. The resultant images contained fringes that are deceptively like one- and two-dimensional lattice fringes. These fringes are, however, *not* simply related to the crystal structure of the particle, and "lattice spacings" measured from them will be in error. In addition, depending upon particle orientation, HRTEM images of a perfect nanoparticle can show details that may be erroneously interpreted as "relaxations," "bent planes," and even "twinned" areas.

37770 ■ **Effect of Pre-Aging on the Evolution of Ge Precipitates in an Al-1.8 at % Ge Alloy**

S. Hinderberger, S.-Q. Xiao, K.H. Westmacott and U. Dahmen

Zeits. für Metallk., 87 (3), 161 (1996) 87 161-170 *1996*

The shape distribution of Ge precipitates in a quenched and aged Al-1.8% Ge alloy was characterized by transmission electron microscopy. In agreement with previous investigations, at least six different precipitate morphologies were distinguished: tetrahedra, octahedra and triangular plates all with the cube-cube orientation relationship; as well as laths along <100> Al directions, laths along <110> Al directions, and plates on {100} Al planes, with three different orientation relationships, respectively. The distribution of precipitate shapes was found to depend strongly on the heat treatment schedule. After quenching to 0° C, samples aged at 200° C exhibited predominantly triangular plates and tetrahedra and were insensitive to pre-aging at room temperature. By comparison, samples aged at 250 and especially at 300 C contained mainly lath-shaped precipitates after short pre-aging times, but a sharply increasing fraction of tetrahedra, octahedra and triangular plates for longer pre-aging times. When the temperature of the quench bath was raised from 0 to 40° C, samples aged at 200° C remained unchanged whereas samples aged at 250 and 300° C retained only lath shaped precipitates. Quenching directly to the three aging temperatures changed the precipitate distribution to a coarse array of large {100} plates.

38303 ■ Microscopy Memories

K.H. Westmacott

British Inst. of Materials 309-323 *1996*

This paper, published in "Towards the Millenium: A Materials Perspective," was presented at a meeting in Birmingham University commemorating Professor R.E. Smallman's 65th Anniversary. It traces some aspects of the authors' experiences in transmission electron microscopy over a 40-year span with particular emphasis on the value of collaborative research. The micrographs illustrate the advances that have been made over this period.

39330 ■ Synthesis, Tailored Microstructures and "Colossal" Magnetoresistance in Oxide Thin Films

K.M. Krishnan, A.R. Modak, H. Ju and P. Bandaru

Ceramic Microstructures '96 *(submitted)*

$La_{1-x}M_xMnO_3$ (where M = Sr, Ba or Ca) thin films, exhibiting very high or "colossal" magnetoresistance (CMR), have generated much recent scientific and technological interest . In addition to raising fundamental questions on insulator-metal transitions and magneto-transport phenomenon, these materials have potential impact on the future of magnetic field sensing and data storage devices. However, the magnetic and magneto-transport properties of these manganite thin films are believed to be dependent on the optimization of the conditions of growth/annealing, composition, oxidation state, epitaxy and the overall microstructure.

In order to address these issues we have grown $La_{1-x}M_xMnO_3$ ($0<x<1$) films (LSMO) using both pulsed laser deposition and a polymeric sol-gel route developed in our laboratory. Pulsed laser deposition provides the ability to deposit ultra-thin films (1-10 nm) and multilayers in addition to being an established, albeit slower, method for the synthesis of thicker (100-1000nm) perovskite films. Polymeric sol-gel synthesis, if suitably optimized, is very versatile and inexpensive. It has additional advantages of overall simplicity, low processing temperature, ease of composition variation, and the ability to produce a wide range of structures.

no # ■ **Transmission Electron Microscopy of Al-rich III-V Oxides**

Z. Liliental-Weber, M. Li, G.S. Li, C. Chang-Hasnain, and E.R. Weber

IEEE SIMC-9 159-162 *1996*

Transmission electron microscopy was used for the characterization of microstructure of wet oxidation of AlAs. Dense cubic γ-Al_2O_3 was formed with a substantial shrinking after oxidation. Addition of a small amount of Ga (x=0.1) increased granularity of the oxide. Large pores were formed at the interface between the oxide and the low Al content layer. Arenic accumulation near these pores, the interface, as well as the layer surface was found after oxidation. This study showed that properties of this oxide might be enhanced by the properties of GaAs rich in As (similar to low-temperature-grown-GaAs).

no # ■ **Strain Effects in GaN Thin Film Growth**

J. Krüger, C. Kisielowski, T. Suski, S. Ruvimov, Z. Liliental-Weber, J.W. Ager III, M. Rubin and E.R. Weber

IEEE-SIMC-9 89-92 *1996*

Strain effects in GaN thin film crystals are analyzed by Photoluminescence (PL), x-ray and Raman scattering. All three methods can be consistently used to monitor strain that depends on the choice of substrate and other parameters. The high amount of stress incorporated in GaN hetero-epitaxial samples causes confusion as to assignment of the PL lines of donor bound excitons and donor-acceptor transitions. Homo-epitaxially grown GaN films provide a reference for unstrained films. The PL line positions of the donor accceptor pair transitions are found to exhibit a different stress coefficient than the excitonic line.

no # ■ **Structural Defects in GaN**

S. Ruvimov and Z. Liliental-Weber

IEEE-SIMC-9 85-88 *1996*

Conventional and high resolution electron microscopy has been applied to study defects in both epitaxial and bulk GaN of wurtzite structure. Because of different growth conditions, epitaxial and bulk GaN crystalline materials differ in their defect structures. While stacking faults and dislocation loops associated with precipitates are typically observed in bulk GaN, dislocations are the major defect found in epitaxial GaN layers. Formation of stacking faults is equivalent to a wurtzite-zincblede structure transformation within a few basal planes and, hence, to a local change in symmetry.

39206 ■ **Automation for On-line Remote-Control *in situ* Electron Microscopy**

D. Owen, M.A. O'Keefe, B. Parvin, J. Taylor, K. H. Westmacott, W. Johnston and U. Dahmen

Proc.15th Pfefferkorn Conf. *1996*

We are continuing development of a multimedia system for remote operation of transmission electron microscopes and using it to control the Kratos 1500keV HVTEM at the NCEM during *in situ* experiments. Full operational control requires adjustments of external stimuli, adjustment of specimen position and orientation, and manipulation of microscope controls such as illumination, magnification, and focus. In conventional (non-remote) operation, a local operator makes adjustments in response to the image from the microscope; in remote mode, current wide area networks cannot offer the real-time delivery guarantees required for the adjustments necessary for dynamic *in situ* studies.We have designed a system that minimizes the real-time delivery requirement by incorporating local automation of stage control and microscope focus. The system corrects for specimen drift (often severe during rapid heating and cooling) by controlling stage movement with optical flow fields; it provides automatic focus using wavelet coefficients with Dauberchies kernels.

39205 ■ TEM Analysis of the Properties of Dislocations in Electronic Materials

F.M. Ross and R. Hull

Proc. 3rd Cong. Mex. Mic. *(in press)* 1996

In this paper we describe a study of the electrical properties of defects in SiGe/Si p-n junction diodes. The defects examined are misfit dislocations, formed at the SiGe/Si interface during growth and subsequent processing and driven by the lattice mismatch between the GeSi and Si. Previous studies of the relationship between dislocations and device performance have generally relied on a statistical correlation between performance and dislocation density over many devices . In the experiments we describe here, the electrical characteristic of an individual diode is measured and correlated with the dislocation density within that particular device. The measurements are repeated as additional dislocations are introduced by heating the device *in situ*. This technique provides information about the kinetics of dislocation formation as well as about the electronic properties of the dislocations themselves.

39188 ■ Epitaxial Magnetic Garnet Heterostructures

R. Ramesh, B. Simion, G. Thomas

Proc. 7th Int'l Conf. on Ferrites 1 *1996*

A summary of our recent progress in the growth and characterization of magnetic and magneto-optic garnet heterostructures is presented in this paper. The similarity in crystal chemistry and lattice parameters among the various garnets (yttrium iron garnet, bismuth iron garnet, etc.) is utilized to create artificially layered heterostructures and superlattices. Rare earth (especially Eu) substitutions in the Bi site are shown to dramatically improve the magneto-optic response and change the easy axis from in-plane to out-of-plane. Microstructural studies indicate that the interface roughness is dependent on the thicknesses of the different layers suggesting the possible role of lattice mismatch induced stresses in surface roughening.

no # ■ **HRTEM and TEM Simluations on a Personal Computer with SIMPLY-S**

T. Epicier, M.A. O'Keefe

Proc. Eur. Cong. Elec. Mic. 1 *1996*

Interpreting high resolution transmission electron microscopy (HRTEM) studies in materials sciences requires the assistance of image simulations. Although numerous packages are today available to run such calculations, none of them is devoted to the PC-compatible computers. The present set of programs SIMPLY-SHRLI, or SIMPLY-S (SIMulation and disPLaY of TEM and HRTEM images - Simulation of High Resolution Lattice Images) has been developed for such personal computers, taking care that ordinary configurations and peripherals are sufficient to perform any calculation (DOS application, which can be run from Windows 3.1 or Windows 95, VGA display, Postscript output files). SIMPLY-S uses a graphical user interface (GUI) to run the multislice-based SHRLI package for simulation of HRTEM micrographs. For an illustration of the dynamical calculations, the reader is referred to the recent 'Round Robin test' of simulation programs, where SIMPLY-S results are compared with results obtained from other commercial and non-commercial packages (WWW site http: //www.ruca.ua.ac.be/~modb).

no # ■ **Application of Cross-Correlation Technique for the Analysis of Fresnel Effect in Small Particle HREM Imaging**

V. Radmilovic, R. Kilaas, M.A. O'Keefe

Proc. Eur. Cong. Elec. Mic. 1 *1996*

Analysis of Fresnel contrast visible at the edges of nanoparticles in the high resolution electron microscope provides a valuable tool for determining the size of the particles with near-atomic-spacing accuracy. We have used HRTEM image simulation to explore the changes in images of a nanoparticle under various imaging conditions, in particular to relate the model particle size and its apparent size as derived from the HRTEM image. The minimal difference between particle and apparent sizes is obtained at a defocus approximately 400Å below the Gaussian image plane, i.e. close to the Scherzer value for the JEOL ARM 1000 of $\sqrt{(CS)}$ = 448Å. At nearly all defocus settings above and below the Scherzer defocus, the spot intensity distribution does not correspond to the positions of the atoms in the particle, especially near a thick edge, leading to an apparent "relaxation" of atom positions near the particle edge. This effect is due to a strong Fresnel influence on the image, since the deviations between atoms and dots are more pronounced in regions close to the thick edges of small particles, i.e. in regions where the potential drop is sharper and the Fresnel fringe more intense. Apparent "relaxation" has been measured by cross-correlating apparent atom positions near the particle edge with those near the center of the particle.

38548 ■ Telepresence for In Situ Electron Microscopy

B. Parvin, J. Taylor, B. Crowley, L. Wu, W. Johnston, (ICSD), D. Owen, M.A. O'Keefe and U. Dahmen

Proc. IEEE Conf. *(in press)* 1996

We present an approach for remote operation of instruments in the Internet environment. We have applied this approach to in-situ electron microscopy experiments that require dynamic interaction with the specimen under observation, as it is excited with external stimuli. Dynamic operations include control of the sample's position and orientation under the electron beam, illumination conditions and focus. We suggest that an effective approach to remote operation for this class of dynamic control applications must involve *automated* control operations performed *near* the instrument in order to eliminate the wide area network real-time delivery requirement. Our approach to this problem is based on advanced computer vision algorithms that permit instrumentation adjustments to be made in response to information extracted from the video signal generated by the microscope imaging system.

37619 ■ TEM Characterization of Invariant Line Interfaces and Structural Ledges in Mo-Si Alloy

S.Q. Xiao, U. Dahmen, S.A. Maloy and A.H. Heuer

Proc. iib'95 Mat. Sci. Forum 207-209 117-120 *1996*

Two distinct <110> lath morphologies of Mo_5Si_3 precipitates observed in $MoSi_2$ differ in their cross-sectional shape and lattice orientation. Type I laths exhibit a rectangular cross section, with interfaces parallel to low-index planes, while type II laths are parallelogram-shaped, with their major interface at 13° to the type I precipitate. The corresponding orientation relationships differ by a 1.8° rotation around the lath axis. In this study, the difference between the two characteristic morphologies and orientation relationships is shown to be the formation of an invariant line strain for type II precipitates. On an atomic scale, both interfaces have a terrace and ledge structure but differ in the stacking sequence of interfacial ledges associated with partial dislocations. The structural unit model and the invariant line model predict identical interface geometries which agree closely with the observations.

37912 ■ Misfit Dislocations Associated with Ultrathin Twins Along a Ni_3Al/Ni_3Nb Interface

R. Bonnet, M. Loubradou, U. Dahmen and S. Hinderberger

Proc. iib'95 Mat. Sci. Forum 207-209 201-204 *1996*

Typical defects of a Ni_3Al ($L1_2$)/Ni_3Nb (Do_a) faceted interface associated with the orientation relationships (11-1) Ni_3Al // (010)Ni_3Nb and [1-10] Ni_3Al // [100]Ni_3Nb are reported. High resolution electron microscopy reveals the presence, along the same interface, of ledges separating facets with different atomic structures. Some facets are associated with certain interfacial thicknesses since their structures involve one planar fault or an intermediate ultrathin Ni_3Al crystal. The observed ledges are associated with a misfit dislocation (MD) with $\mathbf{b}$ = (-1/6)[113]Ni_3Al. This vector is determined from the comparison of the experimental and simulated images. The multislice method has been applied with atom boxes which account for the elastic field surrounding each misfit dislocation core.

38466 ■ Transmission Electron Microscopy of Advanced Materials

G. Thomas

Proc. IX Conf. E. M. of Solids 3-10 *1996*

We live and work in a world that depends on materials and their performance. The science of materials has developed to a position of great understanding, such that materials can be microscopically tailored to provide specific sets of properties.The practical applications of newly designed materials depend on market interest and costs. In the final analysis it is the processing of materials that remains the key factor. In order to facilitate technical advances, the relationships between processing, microstructure, and performance must be established. This task is generic to all materials whether for mechanical or physical property goals. Central to such understanding is the role played by electron optical, diffraction and analytical methods of characterization in their specificity to synthesis almost to the atomic level.1-3 This paper provides some examples of such applications, and attempts to indicate the generic nature of many problems to be solved.

No # ■ **In-situ TEM examination of crystallization process in amorphous FE-Si-B melt spun alloys**

J. Kusinski, G. Thomas

Proc. IX Conf. Elec. Mic. Solids 339-342 *1996*

In-situ TEM was applied to analyze the dynamic microstructural evolution during annealing. Studies showed iron borides crystallized first at the temperature range 235-270°C, depending on the applied heating rate. The higher the heating rate, the higher the nucleation temperature. At about 320- 340°C, „star-like" and „butterfly-like" $(Fe\text{-}Si)_a$ crystals, probably surface nucleated, begin to precipitate. This was also confirmed by ex-situ examination. The SAD and high resolution image analyses showed that the $(Fe\text{-}Si)_a$ crystal arms grow in the [100] direction.

37580 ■ **In Situ Observation of an Electrochemical Etching Reaction in Silicon**

F.M. Ross and P.C. Searson

Proc. MRS 404 69-74 *1996*

We are attempting to observe the kinetics of an electrochemical etching process by allowing the reaction to occur in real time within the electron microscope. We have designed and constructed a specimen holder for a JEOL 200CX microscope featuring a sealed reservoir which can be filled with an electrolyte. By observing the dynamics of the process, for example as a function of current density, we hope to understand the formation mechanism and to control the morphology of the pores produced. we will describe the progress of the experiments and present images showing the propagation of the etching front.

37394 ■ **Epitaxy and Magnetotransport Properties of $La_{0.8}Sr_{0.2}MnO_3$ Films Synthesized by Both Pulsed Laser Deposition and Novel Chemical Routes**

A.R. Modak and K.M. Krishnan

Proc. MRS 401 443-448 *1996*

$La_{0.8}Sr_{0.2}MnO_3$ thin films with different microstructural characteristics were prepared by both pulsed laser deposition and a novel polymeric sol-gel process. For both techniques, polycrystalline films were obtained on Si(100) with a native oxide surface but epitaxial and highly oriented growth could be induced on lattice-matched $LaAlO_3$(100) substrates. While the overall magnetization and magnetoresistance behavior as a function of temperature and applied field were consistent with recent results, i.e., a semiconductor-to-metal transition accompanied by an antiferromagnetic- to-ferromagnetic transformation and large magnetoresistance at the resistance peak temperature, the properties of the films were significantly different depending on the microstructure, epitaxy and polycrystallinity. Detailed microstructural characterization of the films are presented and correlated with their magnetic/magnetotransport properties.

38159 ■ **Structural Defects in Heteroepitaxial and Homoepitaxial GaN**

Z. Liliental-Weber, S. Ruvimov, C. Kisielowski, Y. Chen, W. Swider, J. Washburn, N. Newman, A. Gassmann, X. Liu, L. Schloss, et al

Proc. MRS 395 351-362 *1996*

The microstructure and characteristic defects of heteroepitaxial GaN films grown on sapphire using MBE and MOCVD methods and of homoepitaxial GaN grown on bulk substrates are characterized by TEM, x-ray diffraction, and cathodoluminescence. The difference in arrangement of dislocations along grain boundaries and the influence of buffer layers on the quality of epitaxial films is described. The structural quality of GaN epilayers is compared to that of bulk GaN crystals grown from dilute solution of atomic nitrogen in liquid gallium. Homoepitaxial films grown using MOCVD showed the best quality and were almost free from extended defects. For the bulk GaN crystals a substantial difference in crystal perfection was observed near opposite c-faces of the plates. On one side the surface was almost atomically flat, and the underlying material was free of any extended structural defects, while the other side was rough, with a high density of planar defects. This difference was related to the polarity of the crystal. A large difference in crystal stoichiometry was also observed within different sublayers of the crystals. Based on convergent beam electron diffraction and cathodoluminescence, it is proposed that GaN antisite defects are related to the yellow luminescence observed in these crystals.

38652 ■ **Effect of Si Doping on the Structure of GaN**

Z. Liliental-Weber, S. Ruvimov, T. Suski, , J.W. Ager III, W. Swider, Y. Chen. C. Kisielowski, J. Washburn, I. Akasaki, H. Amano, C. Kuo, and

Proc. MRS 423 *1996*

The influence of Si doping on the structure of GaN grown by metal-organic chemical-vapor deposition (MOCVD) has been studied using transmission electron microscopy (TEM), x-ray diffraction and Raman spectroscopy. Undoped and low Si doped samples were compared with samples of increased dopant concentration. In addition, defect reduction due to different buffer layers (AIN and GaN) is discussed. Silicon doping improves surface morphology and influences threading dislocation arrangement. High doping leads to a more random distribution of dislocations. Based on this study it appears (for some dopant concentration) that an AIN buffer layer can significantly reduce the number of threading dislocations, leaving the samples more strained. However, no significant reduction of threading dislocations could be observed in the samples with GaN buffer layer. These samples are the least strained.

---

no # ■ **Structural and Optical Properties of Homoepitaxial GaN Layers**

J.M. Baranowski, Z. Liliental-Weber, K. Korona, K. Pakula, R. Stepniewski, A. Wysmolek, I. Grzegory, G. Nowak, S. Porowski, B.

Proc. MRS *1996*

The review of structural and optical properties of homoepitaxial layers grown by MOVCD on single crystals GaN substrates is presented. The TEM technique is used to characterize the structural properties of epi-layers. It is found that the structural properties of GaN homoepitaxial layers are determined by the polarity of the substrate surface on which the growth takes place. It is shown that threading dislocations are present only in the layers grown on the [0001] "smooth" surface. On the other hand the layers grown on the [0001] "rough" surface are free from vertical defects. The characteristic feature of the growth on the "rough" surface are pinholes. The optical properties of homoepitaxial layers are predominantly determined by the growth polarity as well. It is shown also that the reflectivity measurement is the most precise way to determine the exciton energies and that emissions due to free excitons are strongly affected by polariton effects.

39352 ■ Atomic Structure of Interfaces in Mazed Au Bicrystals

C.J. Hetherington, U. Dahmen and J.M. Penisson

Proc. MRS (*submitted*) 1996

Thin films of Au deposited on 111 or 100 Ge substrates can grow in two or more crystallographically equivalent orientations. On removal from the substrate and after annealing, the Au bicrystal film appears as a maze of domains with faceted boundaries. The high density of edge-on interfaces in the films make them ideally suited to electron microscopy, and in the 111 orientation, the 1.44Å spacing of the lattice planes tests the high resolution capabilities of the latest microscopes. The shifts and rotations of the Au lattice across the facets have been studied using newly developed image analysis software. Where the relative displacements of the lattice differ between neighboring facets, the defect that must be present at the facet junction has been characterized.

38823 ■ Remote On-line Control of a High-Voltage In Situ Transmission Electron Microscope with a Rational User Interface

B. Parvin, M.A. O'Keefe, J. Taylor, D. Owen, B. Crowley, K.H. Westmacott, W. Johnston and U. Dahmen

Proc. MSA 384-385 *1996*

Remote on-line electron microscopy is rapidly becoming more available as improvements continue to be developed in the software and hardware of interfaces and networks. As implementations of on-line transmission electron microscopy become more widespread, it is essential that suitable standards be developed and followed. The rational graphical user interface we present here is based on experience gained with a full-function materials science application providing users of the NCEM with remote on-line access to a 1.5MeV Kratos EM-1500 in situ high-voltage transmission electron microscope via existing wide area networks. We have developed and implemented a set of tools, protocols, and interfaces to run the Kratos EM-1500 on-line for collaborative research. The standardized user interface displays the frequently-used controls for magnification, apertures, objective focus and specimen tilt, with a 640x480 window for standard NTSC video. We have found that driving the microscope with the standardized remote user interface greatly eases the user's tasks, leaving him/her free to concentrate on the science rather than the mechanics of running the microscope.

38824 ■ HRTEM Investigation of the Interface between AlN and SiC

M.A. O'Keefe, F.A. Ponce and E.C. Nelson

Proc. MSA 122-123 *1996*

Epitaxial thin films of the group III nitrides play an important role in the fabrication of high-efficiency light emitting diodes. Growth of such films on sapphire requires the use of low temperature buffer layers of AlN or GaN. Silicon carbide has a much closer lattice parameter match than sapphire to AlN, and promises to produce better AlN layers. Since the atomic arrangement at the interface between AlN and SiC determines the degree of perfection of the epitaxial layer, we have attempted to determine the structure of this interface by high-resolution transmission electron microscopy. Devices were grown by MOCVD; AlN was deposited on the Si-face of a-6H SiC, followed by GaN. The specimen was cut for HRTEM observation in the <11bb20> SiC projection. Images were obtained at a specimen thickness of 85Å using the NCEM JEOL ARM-1000 operated at 800keV. Defocus was -1050Å at which the important spacings from both SiC and AlN are passed with the same phase. Four possible interface models were constructed. Model A has Al-C bonding; model B has Si-N; model C has N-C; model D has Si-Al. Comparison of experimental and simulated images shows that C-N and Si-Al bonds are not present at the interface, and that Si-N and C-Al bonding cannot be distinguished under the experimental conditions.

39367A ■ The Impact of Imaging Technologies in Materials Engineering

R. Gronsky

Proc. MSA 6-7 *1996*

Materials Engineering is widely acknowledged as a "hyper-discipline" spanning the fundamental sciences (Physics, Chemistry and Biology) with all of the traditional engineering pursuits (Civil, Electrical, Mechanical, Metallurgical, Nuclear...). A healthy materials engineering program in fact demands interaction among basic science and technology, all classes of materials, and the intrinsic elements of the field, parochially known as properties, performance, structure (including composition) and synthesis (including processing). Advanced characterization techniques are obviously critical to this integration, and new imaging technologies have accelerated the process of characterizing materials at all relevant length scales, communicating large data sets to practicing engineers, and refining manufacturing methods with image-based technologies. The importance of imaging technologies was forecast by the National Research Council in a highly regarded 1989 report "Material Science & Engineering for the 1990's: Maintaining Competitiveness in the Age of Materials," which included prominent mention of all microscopy methods. Since then, the success and challenges associated with imaging technologies have increased dramatically.

39369 ■ Techniques for Quantitative HREM Analysis of Structure and Displacements at Interfacial Steps, Facets and Facet Junctions

U. Dahmen, S. Paciornik, D. Michel and M. Hÿtch

Proc. MSA 102-103 *1996*

Quantitative High Resolution Electron Microscopy (QHREM) has made considerable recent advances in the analysis of localized atomic structure, especially in flat, periodic interfaces. This is largely due to the increased speed and sophistication of computer algorithms that compare experimental and simulated images, and to strategies for refining this comparison. However, defects such as dislocations, disclinations or steps often lead to elastic distortion fields in the experimental image that are not included in the simulations of an idealized interface. In the presence of such defects, it is difficult to separate the short-range atomic structure immediately at the core of the interface from the longer-range displacement fields due to steps and dislocations.

39371 ■ Equilibrium Shapes of Pb Inclusions at 90° Tilt Grain Boundaries in Al

E. Johnson, U. Dahmen, S.-Q. Xiao and A. Johansen

Proc. MSA 364-365 *1996*

Ion implantation of lead in Aluminum leads to spontaneous phase separation and formation of dense distributions of nanosized lead inclusions. The inclusions have fcc structure, and despite the large lattice mismatch (a_{Al}=0.4048 nm and a_{Pb}=0.495 nm) they grow in parallel-cube topotaxy with the matrix. Their shape is cuboctahedral with larger {111} facets and smaller {100} facets which is the minimum-energy shape for an fcc crystal in equilibrium with its vapor, as calculated by considering only nearest neighbor bonds. Implantation of polycrystalline aluminum films is accompanied by preferential nucleation and enhanced growth of inclusions in the grain boundaries. In adapting their equilibrium shape, grain boundary inclusions will be subject to a larger number of constraints than inclusions in the bulk matrix. This may result in a variety of morphologies characteristic for different types of grain boundaries.

39372 ■ A Scalable Approach to Teleoperation

J. Taylor and B. Parvin

Proc. MSA 388-389 *1996*

Due to the fast pace of computer instrumentation and technology, we are quickly approaching an age where on-line use of expensive research facilities will become commonplace. The consequences of this trend will be multifaceted. It will allow scientist and researchers to perform experiments and access data with greater ease without the burdensome overhead associated with working onset. It will allow for the on-line storage and analysis of data. And lastly, an ideal testbed will be provided for integrating intelligent man-machine interfaces in order to reduce labor intensive tasks. This will simplify the control of complicated instruments via automation of the controls whose human control is not essential. Based on the experience of building on-line systems for use of optical and electron microscopes, we propose a scalable system architecture based on the principles of object oriented design and analysis, a machine independent user-interface based on Java, and a software but that supports distributed objects over the network.

39373 ■ On the Crystallography of Triple Points in Nonoxide Ceramics: Epitaxial Relationships are a Function of Statistics and Geometry

W.J. Moberly Chan

Proc. MSA 648-649 *1996*

Covalent ceramics, such as SiC and Si_3N_4, can have superior mechanical properties for high temperature structural materials. However, densification difficulties and poor fracture toughness have hindered use. Traditionally, the choice of sintering additives has been a "hit and miss" method to improve properties. The primary purpose of an additive is to provide good density, as residual pore size relates to critical flaw size. Another feature of an additive has recently been to invoke fracture around the matrix grains, thereby enhancing toughness. Most reported nonoxide ceramics include upwards of 10% secondary phase(s) as a continuous phase between many matrix grains and causing poor high temperature strength. Even when this secondary phase is crystallized, thin amorphous interfaces are observed. The ABC-SiC processed for this study incorporates <5% total Al, B, and C as additions. The Al enhances densification, as well as the ß-to-å phase transformation at lower temperatures (1600-1900°C); and controlling the microstructural development has provided record toughness.

39374 ■ The ß -3C to å -4H Transformation in SiC with Al, B, and C Additions: Kinetics Dominated by Growth Akin to Ostwald Ripening

W.J. Moberly Chan, J.J. Cao, J.J. and L.C. DeJonghe

Proc. MSA 658-659 *1996*

The cubic-to-hexagonal phase transformation upon heating SiC has been a focus and/or precondition of hundreds of research studies. In single (or large) crystal SiC, partial dislocation motion propagates stacking faults to invoke the transformation, analogous to the classic FCC-HCP transformation in Co. The hexagonal phase can exist in >200 different stacking modulations of planes of Si-C tetrahedra, with the å -6H polytype regarded as the high temperature equilibrium phase. ("6" is the repeat stacking in a unit cell.) The propensity of stacking faults in all SiC materials provide the nuclei for the transformation. Most transformation studies of polycrystalline SiC cite the work of Heuer, et al., which describes a transformation similar to that in single crystals. The Heuer model incorporates grain growth by observing the nucleated alpha phase as sandwiched between "sheaths" of beta phase, with the sheaths continuing to grow and "protect" the growing alpha phase throughout the transformation. Grain growth incurred during processing is typically treated as kinetically independent of the transformation.

39375 ■ Controlling Microstructural Evolution to *In Situ* Toughen and Strengthen Silicon Carbide

W.J. Moberly Chan, J.J. Cao and L.C. DeJonghe

Proc. MSA 692-693 *1996*

Nonoxide ceramics are desirable for high temperature structural applications, however, they have typically exhibited inferior room temperature fracture toughness. Similar to processing developments to toughen Si_3N_4, SiC has recently been processed via control of a phase transformation to produce *in situ* toughened microstructures. An elongated grain shape, coupled with a tortuous fracture path around grains, can provide bridging behind an advancing crack tip, which increases the crack resistance (rising R curve) and halts crack propagation. Most *in situ* toughened nonoxide ceramics incorporate upwards of 10-20% secondary phase(s), which simplifies crack propagation through this weaker phase to improve toughness, but typically at the expense of substantially reducing strength at high temperatures. The ABC-SiC in this study can be processed with <3% secondary phases and consequently exhibits record toughness and higher strength than commercial (Hexology SA) SiC.

39368A ■ Superstructures and Ordering Phenomena in Ceramic Superconductors

R. Gronsky

Proc. MSA 710-711 *1996*

It is now well established that the phase transformation behavior of $YBa_2Cu_3O_{6+\partial}$ is significantly influenced by matrix strain effects, as evidenced by the formation of accommodation twins, the occurrence of diffuse scattering in diffraction patterns, the appearance of tweed contrast in electron micrographs, and the generation of displacive modulation superstructures, all of which have been successfully modeled via simple Monte Carlo simulations. The model is based upon a static lattice formulation with two types of excitations, one of which is a change in oxygen occupancy, and the other a small displacement of both the copper and oxygen sublattices. Results of these simulations show that a displacive $\sqrt{2}$ X $\sqrt{2}$ superstructures forms very rapidly in a morphology of finely textured domains, followed by domain growth and a more sharply defined modulation wavelength, ultimately evolving into a strong <110> tweed with a 5nm to 7nm period. What is new about these findings is the revelation that both the small-scale deformation superstructures and coarser tweed morphologies can result from displacive modulations in ordered $YBa_2Cu_3O_{6+\partial}$ and need not be restricted to domain coarsening of the disordered phase.

38530 ■ Structure of III-V Oxides

Z. Liliental-Weber, M. Li, G.S. Li, C. Chang-Hasnain and E.R. Weber

Proc. MSA 942-943 *1996*

The lack of high-quality native oxides on the III-V compounds has hindered the development of III-V integrated circuits and optoelectronic technology. Recently it was shown that stable oxides can be formed into the III-V compounds rich in Al, such as $Al_xGa_{1-x}As$ with H_2O vapor (in N_2 carrier gas) at elevated temperatures (~400-450°C). The high quality of these oxides was attributed to the formation of stable AlO(OH) and Al_2O_3 compounds. However, this conclusion was not definitive, since several Al rich compounds were proposed as well. In addition, it was never clarified whether the excess As created in this process has any role in the stabilization of these oxides, in reducing leakage current or in impurity diffusion. Moreover there is concern as to the quality of the oxide/GaAs interfaces created by lateral oxidation of an intermediate AlGaAs layer.

39376 ■ In Situ TEM Observations of Melting in Nanosized Eutectic Pb-Cd Inclusions Embedded in Al

S. Hagège, U. Dahmen, E. Johnson, A. Johansen and V.S. Tuboltsev

Proc. MSA 986-987 *1996*

Small particles of a low-melting phase embedded in a solid matrix with a higher melting point offer the possibility of studying the mechanisms of melting and solidification directly by in-situ observation in a transmission electron microscope. Previous studies of Pb, Cd and other low-melting inclusions embedded in an Al matrix have shown well-defined orientation relationships, strongly faceted shapes, and an unusual size-dependent superheating before melting.

39377 ■ GPB Zones as a Precursor for S'Precipitation in Al-Based Matrices

V. Radmilovic, S. Ratkovic, G.J. Shiflet and U. Dahmen

Proc. MSA 996-997 *1996*

In the pseudo-binary Al-Al_2CuMg alloy, the Cu/Mg-rich precipitation zones (GPB) are able to cause considerable hardening of the matrix. The hardening is apparently not very sensitive to the zone size or degree of ordering. According to Silcock these zones are cylindrical, 1-2 nm in diameter and 4 nm long. They are also formed during the early stage of aging at 190°C and are followed by nucleation of Sæ precipitates with {210} habit plane. Overaging occurs by the further formation and growth of Sæ with a corresponding resolution of GPB zones. Since the discovery of GP zones (reach in Cu) in Al-Cu alloys by Guinier and Preston, the structure of these zones, even at atomic level, has been studied extensively. However, there are very few studies of GPB zone structure and crystallographic relationship with Al matrix. In this paper results using atomic resolution electron microscopy on the GPB zone size, structure and crystallographic orientation relationship with Al matrix are reported.

no # ■ **Design and Implementation of a Site for a One-Angstrom TEM**

J. Turner, M. A. O'Keefe, Robert Mueller

Proc. MSA *(submitted)* 1997

NCEM has recently acquired a field-emission TEM to form the basis of a project to achieve a resolution of one Ångstrom. To reach this resolution, both instrumental and environmental factors need to be considered. We have designed and constructed a new building to provide a suitable environment for this instrument, with emphasis on providing isolation from external influences detrimental to the achievement of ultra-high resolution. The microscope chosen for the one-Ångstrom project is a Philips CM300 Ultra-Twin equipped with a field-emission gun. In order to reduce the effects of external vibration, the CM300UTFEG microscope room was constructed around a specially-constructed slab of reinforced concrete approximately one meter thick and 3.3m by 4.2m. Vibration measurements were carried out using a B&K type 2515 vibration analyzer with a 8318 sensor, as supplied by Philips. It was found that measured vibration levels tracked the storm activity on the Northern California coast. Results of vibration measurements on the slab show significant attenuation of vibration, ensuring that all measured vibrations are well below allowed levels. In the vertical direction, vibration attenuation by the slab is close to a factor of three in the critical range from 1Hz to 5Hz, whereas horizontal attenuation in this range is even stronger and approaches a factor of ten times.

---

no # ■ **Al-based Thermal Oxides in Vertical Cavity Surface Emitting Lasers**

Z. Liliental-Weber, S. Ruvimov, W. Swider and J. Washburn

SPIE, Int. Soc.Opt. Eng. 3006 15-25 *1997*

The microstructure of wet oxidized layers for vertical cavity surface emitting lasers (VCSELS) was studied by transmission electron microscopy. These oxides were formed by reaction of $Al_xGa_{1-x}As(x\sim0\text{-}0.2)$ with H_20 vapor at elevated temperatures (~400-450∞C). Due to the excellent carrier confinement provided by the oxidized layer, VCSELS have very low threshold currents and high efficiencies. This study revealed the accumulation of excess As at the interfaces with the oxidized layers and occasionally at the sample surface. To avoid this As accumulation on the sample surface, GaInP layers were grown on top of AlGaAs/GaAs layers. In this case no As was found at the layer surface. In addition, substantial shrinkage was found after oxidation, and the formation of large pores at the interface between the oxide and the high Al content layer, which might be detrimental for the device performance. The dependence of the oxide and interface quality on the composition of the oxidized layers, oxidation time and temperature are discussed in relation to the optical quality of VCSELS.

39284 ■ **Structure and Device Characteristics of $SrBi_2Ta_2O_9$ Memories**

J.F. Scott, F.M. Ross, C.A. Paz de Araujo, M.C. Scott and M. Huffman

MRS Bulletin *1996*

Electron micrographs of the layer-structure perovskites ($SrBi_2Ta_2O_9$) that have become the materials of choice for non-volatile computer memories [Paz de Araujo et al., Nature 374, (1995) p. 627] reveal very complicated structures. In bulk form this family of materials exists primarily in a structure with two TaO_6 octahedra interrupted by Bi_2O_2 planes. The thin-film forms are complicated, with amorphous regions and second phases. Mechanisms of leakage current and electrical breakdown in these materials are discussed.

Please send a reprint of the paper(s):

Number	First Author	Title (first two words)

Name_____ Date_____

Affiliation _____

Address _____

_____

Please send a reprint of the paper(s):

Number	First Author	Title (first two words)

Name_____ Date_____

Affiliation _____

Address _____

_____

National Center for Electron Microscopy
Berkeley Laboratory
1 Cyclotron Rd., Building 72
Berkeley CA 94720

National Center for Electron Microscopy
Berkeley Laboratory
1 Cyclotron Rd., Building 72
Berkeley CA 94720

☆ U.S. GOVERNMENT PRINTING OFFICE: 1997-584-600/P3144

National Center for Electron Microscopy
Ernest Orlando Lawrence
Berkeley National Laboratory
University of California
Berkeley, CA 94720